Electronic Supplementary Material (ESI) for Inorganic Chemistry Frontiers.

Introducing Anthracene and amino groups into Ln-OFs Photo-reduction of Cr(VI) Without Additional Photosensitizers and Cocatalysts

Wenxiao Guo, [a‡] *Shufang Wang,* [a‡] *Hongguo Hao,* [a*] *Xiangjin Kong,* [a] *Hui Yan,* [a] *Hongjie Zhu,* [a] *YunWu Li,* [a] *Huawei Zhou,* [a] *Dichang Zhong,* [b*] *Fangna Dai* [c]

[a]Shandong Provincial Key Laboratory of Chemical Energy Storage and Novel Cell Technology, School of Pharmacy, School of Chemistry and Chemical Engineering, College of Materials Science and Engineering, and Dongchang College, Liaocheng University, Liaocheng 252059, China.

[b]Institute for New Energy Materials and Low Carbon Technologies School of Materials Science and Engineering Tianjin University of Technology Tianjin 300384, China.

[c]College of Science, School of Materials Science and Engineering, China University of Petroleum (East China), Qingdao, Shandong 266580, China.

‡ Wenxiao Guo and Shufang Wang contributed equally to this work.

* Corresponding Authors, E-mail: hhg207@126.com; dczhong@email.tjut.edu.cn

Supplementary Information

Contents

1. Experimental Section 3

2. Crystal structure and IR and PXRD of LCUH-100 5

3. Photocatalytic Cr(VI) reduction properties characterization. 8

1. Experimental Section

1.1 Materials and Methods. All reagents and solvents were obtained commercially and used without any purification. Crystal data were obtained from a Rigaku Oxford Diffraction Gemini diffractometer, equipped with a Mo *K*α with *ω*-scan technique. The powder X-ray diffraction patterns (PXRD) were recorded on a Rigaku D/Max-2500 diffractometer and the intensity data were recorded by continuous scan in a 2*θ* mode from 5 to 50°, with a step size of 0.1 and a scan speed of 20 min^{-1}. A PerkinElmer Diamond SII thermal analyzer was utilized for Thermo gravimetric analysis (TGA) tests from 298 to 1073 K, at a heating rate of 10 K min^{-1} under a nitrogen atmosphere. Infrared spectra were recorded on a Nicolet 6700 FT-IR spectrophotometer with KBr pellets in the range 4000-400 cm^{-1} region. X-ray photoelectron spectrums (XPS) characterization was carried out by using a Thermo Fisher Scientific ESCALAB spectrometer with Al *K*α X-rays (1486.6 eV) as the light source. UV-visible spectroscopy measurements were conducted with a UH 4150 spectrophotometer. Electron Paramagnetic Resonance Spectrometer (EPR) was conducted on a EPR-200Plus spectrometer. The diffuse reflectance spectra of all the materials were explored by a UV-vis spectrophotometer (Shimadzu UV-3600, Japan) with $BaSO_4$ as a comparison. The Mott-Schottky curves were obtained at a GAMRY references 3000 electrochemical workstation. Photocurrent measurements were performed on a workstation (CHI760E) in a standard three-electrode system configuration with the photocatalyst-coated ITO as the working electrode, Pt net as the counter electrode, and Ag/AgCl as the reference electrode. Photocatalytic reactions were performed on a CEAULIGHT photochemical reactor (CEL-LB70). The Electrochemical Impedance Spectroscopy were carried out using Gamry references 3000 electrochemical workstations, equipped with an electrode rotator (Pine, RDE710). Photoluminescence (PL) emission measurements were conducted using a fluorescence spectrophotometer (Hitachi F-7000, Japan). The time-resolved photoluminescence (TRPL) spectra were measured using an Edinburgh FLS 1000 spectrophotometer. Element distribution was characterized by Hitachi SEM S-4800. Energy-dispersive X-

ray spectroscopy (EDS) and element mapping analyses were recorded on a Thermo Fisher Scientific FIB-SEM GX4. The transmission electron microscopy (TEM) observation was performed on a Jem-2100F electron microscope operating.

2. Crystal structure and IR and PXRD of LCUH-100

Table S1. Crystal Parameters for LCUH-100.

Complex	LCUH-100
CCDC no.	2170346
Empirical formula	$[Sm_4C_{146}N_8O_{30}H_{116}][C_4H_9NO]_3[H_2O]_8$
Formula weight	3469.22
Temperature/K	298.15
Crystal system	triclinic
Space group	*P*-1
a/Å	19.3340(18)
b/Å	20.3749(19)
c/Å	22.104(2)
α/°	90.7600(10)
β/°	93.8540(10)
γ/°	114.234(3)
Volume/Å^3	7914.2(13)
Z	2
ρ g/cm^3	1.395
μ/mm^{-1}	1.536
F(000)	3358
Crystal size/mm^3	0.3 × 0.2 × 0.1
Radiation	Mo *Kα* (λ = 0.71073)
2*θ* range for data collection/°	4.232 to 56.926
Reflections collected	51414
R_{int}	0.0896
Goodness of fit	0.966

Computer programs: *CrysAlis PRO*, Agilent Technologies, *SHELXL*2018 (Sheldrick, 2018), *DIAMOND* (Brandenburg & Putz, 2005) *and publCIF* (Westrip, 2010).

Table S2. Selected Bond Lengths (Å) of LCUH-100.

LCUH-100							
Atom- Atom	**Length/Å**	**Atom- Atom**	**Length/Å**	**Atom- Atom**	**Length/Å**	**Atom- Atom**	**Length/Å**
Sm1-O1	2.568(8)	**Sm2-O3**	2.405(8)	**Sm3- O13^3**	2.351(7)	**Sm4- O12^3**	2.425(8)
Sm1-O2	2.407(10)	**Sm2-O6**	2.455(8)	**Sm3- O14^2**	2.410(8)	**Sm4-O19**	2.416(8)
Sm1-O3	2.739(8)	**Sm2-O7**	2.462(8)	**Sm3- O15^2**	2.430(7)	**Sm4-O20**	2.859(8)
Sm1-O4	2.361(8)	**Sm2-O9**	2.915(9)	**Sm3-O16**	2.511(8)	**Sm4-O21**	2.483(8)
Sm1-O5	2.318(8)	**Sm2-O8**	2.364(11)	**Sm3-O17**	2.433(8)	**Sm4-O27**	2.373(9)
Sm1-O8	2.340(8)	**Sm2-O10**	2.505(11)	**Sm3-O18**	2.393(7)	**Sm4-O26**	2.525(10)
Sm1-O24^1	2.437(8)	**Sm2-O11**	2.463(9)	**Sm3-O19**	2.702(7)	**Sm4-O28**	2.499(7)
Sm1-O25^1	2.461(8)	**Sm2-O22^2**	2.493(8)	**Sm3- O20**	2.357(8)	**Sm4-O32^1**	2.494(8)

Symmetry codes for LCUH-100: ^{1}1-X, 1-Y, 1-Z; ^{2}1-X, 2-Y, 1-Z; ^{3}+X, + Y, 1+Z;

Table S3. Selected bond angles (º) for LCUH-100.

LCUH-100							
Atom-Atom-Atom	Angle/°	Atom-Atom-Atom	Angle/°	Atom-Atom-Atom	Angle/°	Atom-Atom-Atom	Angle/°
O1-Sm1-O3	113.9(3)	O3-Sm2-O6	84.3(3)	O13^{3}-Sm3-O14^{2}	84.5(3)	O12^{3}-Sm4-O20	67.9(3)
O2-Sm1-O1	51.3(3)	O3-Sm2-O7	117.5(3)	O13^{3}-Sm3-O15^{2}	83.0(3)	O12^{3}-Sm4-O21	83.4(3)
O2-Sm1-O3	69.4(3)	O3-Sm2-O8	71.4(2)	O13^{3}-Sm3-O16	165.4(3)	O12^{3}-Sm4-O27	70.2(3)
O2-Sm1-O24^{1}	125.8(3)	O3-Sm2-O10	150.6(4)	O13^{3}-Sm3-O17	142.5(3)	O12^{3}-Sm4-O28	131.6(3)
O2-Sm1-O25^{1}	133.4(3)	O3-Sm2-O11	74.3(3)	O13^{3}-Sm3-O18	81.6(3)	O12^{3}-Sm4-O32^{1}	141.4(3)
O4-Sm1-O1	95.4(3)	O3-Sm2-O22^{2}	134.4(3)	O13^{3}-Sm3-O19	72.9(2)	O12^{3}-Sm4-O33^{1}	147.4(3)
O4-Sm1-O2	87.3(3)	O3-Sm2-O23^{2}	86.5(3)	O13^{3}-Sm3-O20	78.6(3)	O19-Sm4-O12^{3}	80.7(3)
O4-Sm1-O3	51.6(3)	O6-Sm2-O7	81.2(3)	O14^{2}-Sm3-O15^{2}	54.8(3)	O19-Sm4-O20	71.9(2)
O4-Sm1-O24^{1}	136.3(3)	O6-Sm2-O8	67.8(3)	O14^{2}-Sm3-O16	87.7(3)	O19-Sm4-O21	118.6(3)
O4-Sm1-O25^{1}	84.0(3)	O6-Sm2-O10	70.2(3)	O14^{2}-Sm3-O17	123.4(3)	O19-Sm4-O27	148.0(3)
O5-Sm1-O1	171.2(3)	O6-Sm2-O11	134.1(3)	O14^{2}-Sm3-O19	154.8(3)	O19-Sm4-O28	74.7(3)
O5-Sm1-O2	137.1(3)	O6-Sm2-O22^{2}	140.3(3)	O15^{2}-Sm3-O16	82.4(3)	O19-Sm4-O32^{1}	136.3(3)
O5-Sm1-O3	72.1(3)	O6-Sm2-O23^{2}	145.2(3)	O15^{2}-Sm3-O17	132.5(3)	O19-Sm4-O33^{1}	85.9(3)
O5-Sm1-O4	83.2(3)	O7-Sm2-O8	46.8(2)	O15^{2}-Sm3-O19	130.5(2)	O21-Sm4-O20	47.2(2)
O5-Sm1-O8	77.4(3)	O7-Sm2-O10	73.9(3)	O16-Sm3-O19	116.7(3)	O21-Sm4-O27	71.9(3)
O5-Sm1-O24^{1}	87.4(3)	O7-Sm2-O11	73.9(3)	O17-Sm3-O16	51.4(3)	O21-Sm4-O28	73.3(3)
O5-Sm1-O25^{1}	87.1(3)	O7-Sm2-O22^{2}	85.7(3)	O17-Sm3-O19	73.4(3)	O21-Sm4-O32^{1}	85.3(3)
O8-Sm1-O1	110.0(3)	O7-Sm2-O23^{2}	132.3(3)	O18-Sm3-O14^{2}	137.2(3)	O21-Sm4-O33^{1}	128.9(3)
O8-Sm1-O2	75.5(3)	O9-Sm2-O3	81.6(3)	O18-Sm3-O15^{2}	83.4(3)	O26-Sm4-O12^{3}	74.6(3)
O8-Sm1-O3	75.7(3)	O9-Sm2-O6	72.6(4)	O18-Sm3-O16	95.9(3)	O26-Sm4-O19	83.5(3)
O8-Sm1-O4	127.2(3)	O9-Sm2-O7	146.0(3)	O18-Sm3-O17	90.0(3)	O26-Sm4-O20	137.7(3)
O8-Sm1-O24^{1}	91.6(3)	O9-Sm2-O8	133.6(4)	O18-Sm3-O19	51.3(2)	O26-Sm4-O21	145.9(3)
O8-Sm1-O25^{1}	142.0(3)	O9-Sm2-O10	77.0(4)	O20-Sm3-O14^{2}	89.0(3)	O26-Sm4-O27	76.3(4)
O24^{1}-Sm1-O1	87.6(3)	O9-Sm2-O11	140.1(4)	O20-Sm3-O15^{2}	140.8(3)	O26-Sm4-O28	140.4(3)
O24^{1}-Sm1-O3	157.6(3)	O9-Sm2-O22^{2}	100.7(4)	O20-Sm3-O16	113.7(3)	O26-Sm4-O32^{1}	95.8(3)
O24^{1}-Sm1-O25^{1}	52.8(2)	O9-Sm2-O23^{2}	72.8(4)	O20-Sm3-O17	77.6(3)	O26-Sm4-O33^{1}	74.5(3)
O25^{1}-Sm1-O1	84.1(3)	O10-Sm2-O8	110.0(3)	O20-Sm3-O18	126.9(3)	O27-Sm4-O20	107.4(3)
O25^{1}-Sm1-O3	132.0(3)	O10-Sm2-O23^{2}	105.9(4)	O20-Sm3-O19	75.8(2)	O28-Sm4-O20	65.2(2)

Table S4. Calculated solvent-accessible volume (Å^{3}) and Unit volume (Å^{3}) by *PLATON*.

MOF	LCUH-100
Solvent accessible volume (Å^{3})	2043.2 (25.8%)
Unit volume (Å^{3})	7914.1

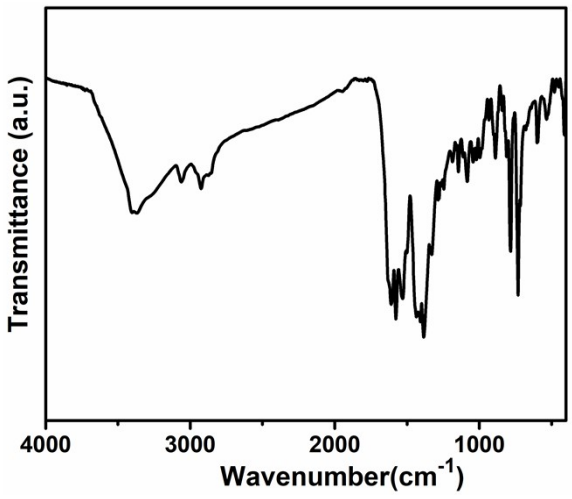

Figure S1. The FT-IR spectral of **LCUH-100**.

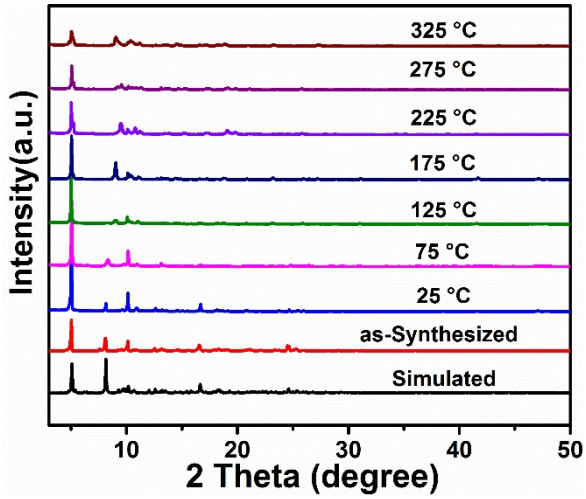

Figure S2. The variable temperature powder test (25°C to 325°C) of **LCUH-100**.

3. Photocatalytic Cr(VI) reduction properties characterization.

Table S5. Energy band calculation of LCUH-100

Catalysts	E_{CB} vs NHE / eV	E_g / eV	E_{VB} / eV
LCUH-100	-1.11	2.85	1.74

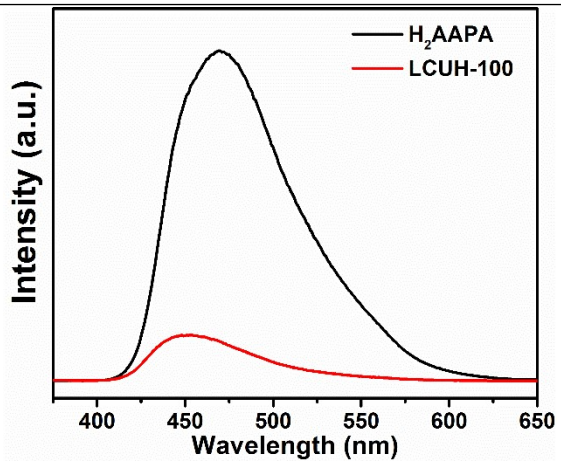

Figure S3. The Steady-state PL spectra of H_2AAPA and **LCUH-100**.

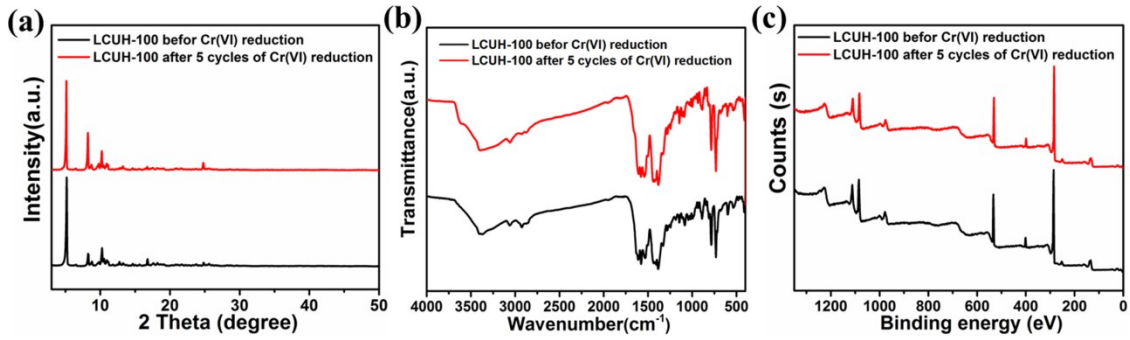

Figure S4. The PXRD patterns (a) IR spectra (b) and XPS spectra (c) before and after 5 cycles of Cr (VI) reduction of **LCUH-100**.

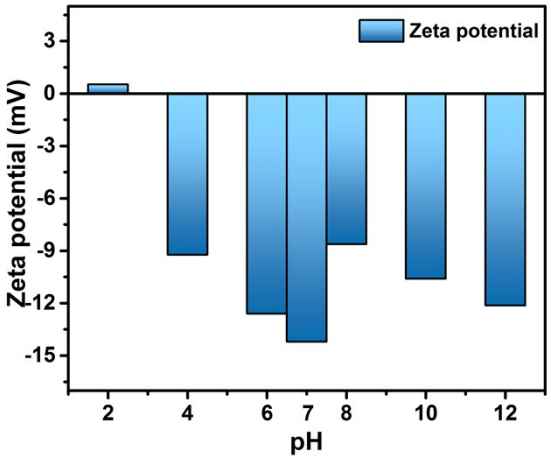

Figure S5. Zeta potentials of **LCUH-100** at different pH values.